Title

Unconventional switching behavior in La0.7Sr0.3MnO3/La0.7Sr0.3CoO3 exchange-spring bilayers

Journal

Applied Physics Letters, 105(20)

ISSN

0003-6951

Authors

Li, Binzhi
Chopdekar, Rajesh V
Arenholz, Elke
et al.

Publication Date

2014-11-17

DOI

10.1063/1.4902115

Peer reviewed

Unconventional switching behavior in $La_{0.7}Sr_{0.3}MnO_3/La_{0.7}Sr_{0.3}CoO_3$ exchange-spring bilayers

Binzhi Li,[1] Rajesh V. Chopdekar,[1] Elke Arenholz,[2] Apurva Mehta,[3] and Yayoi Takamura[1,a)]
[1]*Department of Chemical Engineering and Materials Science, University of California, Davis, Davis, California 95616, USA*
[2]*Advanced Light Source, Lawrence Berkeley National Laboratory, Berkeley, California 94720, USA*
[3]*Stanford Synchrotron Radiation Lightsource, 2575 Sand Hill Road, MS 99, Menlo Park, California 94025, USA*

(Received 28 August 2014; accepted 7 November 2014; published online 17 November 2014)

We report on the observation of exchange-spring behavior in complex oxide bilayers composed of high coercivity ferromagnetic (FM) $La_{0.7}Sr_{0.3}CoO_3$ (LSCO) and low coercivity FM $La_{0.7}Sr_{0.3}MnO_3$ (LSMO). The magnetization process from each individual layer is revealed by a combination of bulk magnetometry and x-ray magnetic circular dichroism measurements. The results show unexpected magnetic switching behavior which deviates from conventional exchange-spring systems in that reversible switching occurs not only within the soft LSMO layer but is also accompanied by the switching of an interfacial LSCO layer. The origin of such exchange coupling is discussed in terms of charge redistribution at the interface. © *2014 AIP Publishing LLC*.
[http://dx.doi.org/10.1063/1.4902115]

Exchange coupling at ferromagnetic/antiferromagnetic (FM/AFM) and FM/FM interfaces has been widely studied over the past few decades due to their applications in various magnetic technologies such as magnetic read heads and high performance permanent magnets.[1–3] FM/AFM interfaces have been found to exhibit exchange bias where the AFM layer pins the soft FM layer at the interface and causes a shift in the hysteresis loop along the field direction. This exchange bias phenomenon has been correlated to factors such as the exchange interactions between the FM layer and uncompensated spins in the AFM layer at the interface as well as magnetic anisotropy in the AFM layer.[1] A similar effect has also been observed at interfaces between hard and soft FM layers, where the hard (soft) layer possesses high (low) coercivity and low (high) saturation magnetization. This exchange-spring behavior enables the synthesis of high performance permanent magnets with optimized $(BH)_{max}$ product.[4,5] Furthermore, the unique magnetization processes of the individual layers[6–8] may have applications in thermally assisted[9] and perpendicular magnetic recording media.[10]

Exchange-spring magnets are usually characterized by the fully reversible switching of the soft FM layer below a critical magnetic field. The hard FM layer is often described as rigid with high anisotropy that pins the magnetic moments of the soft FM layer at the interface. Upon field reversal after saturation, the unpinned moments of the soft phase are free to rotate in a twisting fashion towards an antiparallel alignment with the hard layer and return to a parallel alignment upon field removal.[11] This model has been supported by experimental results in Fe/Sm-Co and Co/Sm-Co systems.[6] However, more complicated switching behaviors were suggested in later studies, where concurrent switching of the soft and hard layers was observed even when the field was well below the nucleation field of the hard layer.[7,12]

While most studies on exchange-spring behavior have been focused on metallic FM alloys, perovskite ABO_3 oxides offer several advantages such as their highly tunable properties through the competition between the charge, lattice, spin, and orbital degrees of freedom,[13] which provide a more versatile route to control interfacial magnetic behavior. For example, novel spin-flop coupling in $La_{0.7}Sr_{0.3}MnO_3$ (LSMO)/$La_{1-x}Sr_xFeO_3$ heterostructures[14,15] and the control of exchange coupling through geometrical confinement have been demonstrated.[16] In addition, exchange-spring-like behavior in $La_{0.67}Sr_{0.33}MnO_3/SrRuO_3$ bilayers showed an antiparallel coupling between the hard and soft layers.[17] It was suggested that this phenomenon was due to electronic reconstruction at the interface via charge transfer that resulted in a change of the Mn-O-Ru bond angle.[17,18] Here, we report the direct observation of exchange-spring behavior in epitaxial (6 nm) LSMO/(6 nm)$La_{0.7}Sr_{0.3}CoO_3$ (LSCO) bilayers, where LSMO is a soft FM material with a coercive field of around 0.002 T and LSCO is a hard FM material with a coercive field of ~0.6 T.[19,20] This isostructural system provides structural continuity across the interface consisting of MnO_6 octahedra stacked epitaxially on top of CoO_6 octahedra. The FM exchange interactions of these perovskites (ABO_3, B: transition metal element) are mediated by the FM superexchange or the double-exchange mechanisms through B-O-B networks.[21] Previously, a strong exchange interaction was observed in (10 unit cell) LSMO/(10 unit cell) LSCO superlattices with a high density of interfaces and thin individual layers,[19] which leads to magnetic switching of the two components as a single unit. The current study on bilayers provides a more detailed examination of a single LSMO/LSCO interface with larger layer thicknesses. Here, the magnetization process is studied using a combination of bulk magnetometry and x-ray magnetic circular dichroism (XMCD) spectroscopy. XMCD provides element-specific magnetic characterization that allows us to probe the magnetization processes

a)Author to whom correspondence should be addressed. Electronic mail: ytakamura@ucdavis.edu.

in the soft and hard layers independently rather than inferring their behavior from bulk magnetometry.

LSMO/LSCO bilayers were grown on (001)-oriented $(LaAlO_3)_{0.3}(Sr_2AlTaO_6)_{0.7}$ (LSAT) substrates with LSCO as the bottom layer by pulsed laser deposition using a KrF excimer laser (248 nm wavelength). During growth, the substrate temperature was held at 700 °C and the oxygen pressure was 0.3 Torr. Laser energies of 0.8 J/cm^2 and 1.0 J/cm^2 were used for the LSMO and LSCO layers, respectively. To assure the proper oxygen stoichiometry, the samples were cooled in 300 Torr oxygen pressure. Single layer LSMO and LSCO films on LSAT were also grown as references. Structural characterization was performed by x-ray diffraction using a Bruker D8 Discover 4-circle diffractometer, and resonant x-ray reflectivity (XRR) measurements were carried out at BL 2-1 of the Stanford Synchrotron Radiation Lightsource (SSRL). The resonant XRR measurements were performed at 8000 eV and at energies near the Mn K edge and Co K edge, where the x-ray fluorescence from the sample just began to rise rapidly, 6556 eV and 7727 eV, respectively.[22] The layer thickness, density, and roughness were determined by fitting the XRR spectra using the Bruker Leptos software.[23] Bulk magnetization was studied using a Quantum Design superconducting quantum interference device (SQUID) magnetometer with the magnetic field applied along the in-plane [100] substrate direction. X-ray absorption (XA) and XMCD spectra were acquired on beamlines 6.3.1 and 4.0.2 of the Advanced Light Source (ALS) in total-electron-yield mode. The applied magnetic field direction was collinear with the x-ray beam that impinged on the sample surface at 60° to the surface normal. All magnetic measurements were carried out at 80 K.

Resonant XRR spectra and the reciprocal space map (RSM) around the (103) reflections of the substrate and films are shown in Figure 1. Clear Kiessig fringes from finite thickness effects are resolved in the three resonant XRR curves and ω-2θ scans around the (002) reflections (not shown) confirm the high crystallinity of the bilayers with smooth surfaces and interfaces. Energy-dependent differences in resonant XRR curves are indicated by arrows in Figure 1 and detailed structural parameters from XRR fitting are tabulated in Table I. For the fitting of XRR spectra, a sample model based on stacking of single layers with abrupt interfaces was used. The cost function listed in Table I is a measure of the logarithmic difference between each experimental and simulated data point and is used as our metric for goodness of fit.[23] The out-of-plane lattice parameters for the LSMO and LSCO layers determined from (002) scans are 0.3892 nm and 0.3802 nm, respectively. RSMs from all four variants of the {103} family of reflections show that the film and substrate peaks are aligned vertically along the (h00) axis with the same relative positions, indicating full epitaxial growth relative to the substrate with 0.6% tensile strain and −1.7% compressive strain for LSMO and LSCO, layers respectively.

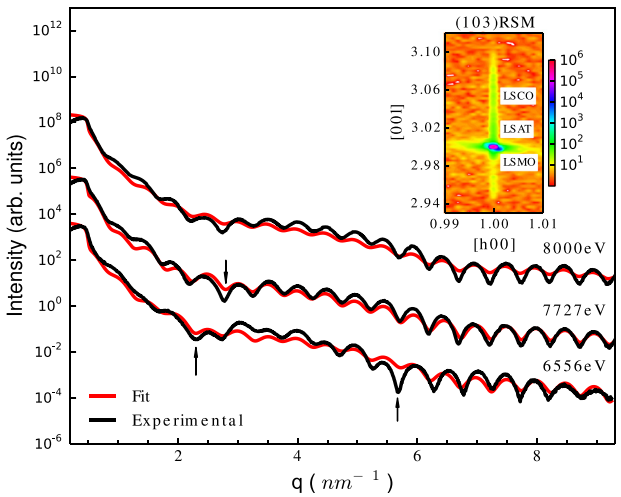

FIG. 1. Measured and fit resonant XRR curves measured at 8000 eV and at energies near the Mn K edge (6556 eV) and Co K edge (7727 eV). Inset shows the RSM of the film and substrate (103) reflections. The arrows indicate additional features in resonant XRR curves.

Figure 2(a) plots the SQUID hysteresis loop for the bilayer where the magnetization consists of contributions from both layers. The hysteresis loop for the single layer LSCO film is included for comparison showing a coercive field of 0.6 T. The linear diamagnetic background from the LSAT substrate has been subtracted. The sample was zero-field cooled from room temperature to 80 K and a major hysteresis loop with H between +/−1.4 T was measured. Upon field reversal from saturation, the major loop exhibited a large drop in magnetization at H = −0.005 T and a smaller gradual drop near H = −0.6 T. The two transitions correspond to the transition fields of the soft (LSMO) and hard (LSCO) layers, respectively. The saturation magnetization (M_s) values at 80 K for the two layers estimated from the hysteresis loop are 490 emu/cm^3 (3.08 μ_B/Mn) for the LSMO layer and 120 emu/cm^3 (0.74 μ_B/Co) for the LSCO layer. The M_s values are comparable with the reported values of single layer LSMO and LSCO films with similar thickness.[24,25]

To probe the exchange-spring behavior within the soft LSMO layer, the samples were biased to either +1.4 T or −1.4 T (to align the hard LSCO layer) and minor hysteresis loops were measured between ±0.4 T (i.e., below the transition field for the LSCO layer). The data from the SQUID major loop have been included as open symbols for comparison. As can be seen in Figure 2(b), the minor loops follow the trace of the major loop with horizontal and vertical shifts along the field and magnetization axes, respectively, depending on the biasing condition. The vertical shift of the minor loops can be attributed to a portion of the bilayer magnetization which remained fixed along the direction of the biasing

TABLE I. Thickness, roughness, and density values obtained from XRR fitting.

	Thickness (nm)	Roughness (nm)	Density (g/cm^3)	Theoretical density (g/cm^3)
Cap layer (carbon)	1.43	0.18	1.19	N/A
LSMO	6.37	0.17	6.43	6.46
LSCO	6.20	0.30	6.30	6.73
LSAT (sub)	N/A	0.03	6.72	6.72[a]
Energy (eV)	6556	7727	8000	
Cost function	6.14×10^{-2}	2.81×10^{-2}	3.56×10^{-2}	

[a]The density of the LSAT substrate was held constant at 6.72 g/cm^3.

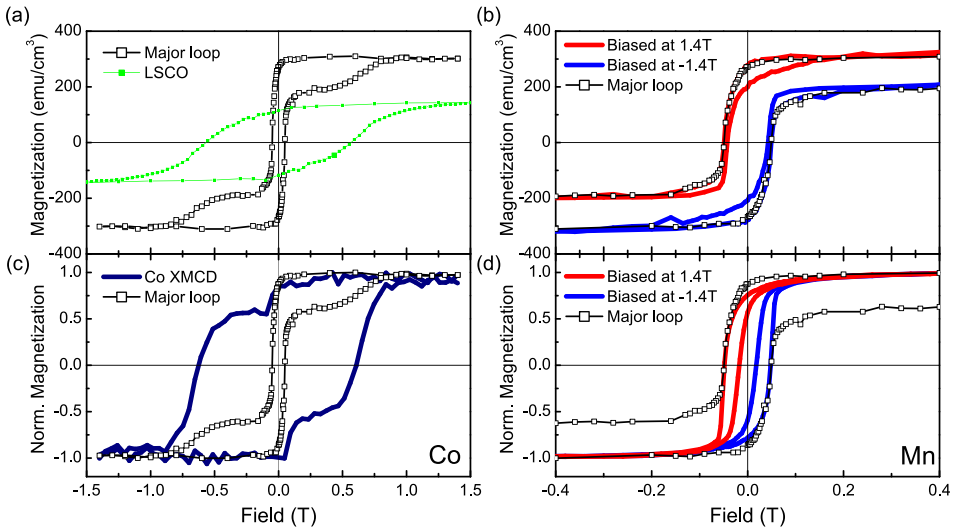

FIG. 2. (a) Major hysteresis loops measured using a SQUID magnetometer for the bilayer (shown in all panels for comparison) and single layer LSCO film; (b) SQUID minor hysteresis loops for the bilayer after biasing at +/−1.4 T; (c) Co edge XMCD major hysteresis loop for the bilayer; and (d) Mn edge XMCD minor hysteresis loop for the bilayer after biasing at +/−1.4 T.

field and was not affected by the sweeping field. The lateral shift of the minor loops was always in the opposite direction of the biasing field. This shift can be attributed to magnetic moments that are fixed and do not follow the external field up to +/−0.4 T. It is generally believed that for exchange-spring systems, the switching behavior of the soft layer is fully reversible with fields below the transition field of the hard layer.[11] The minor loops in Figure 2(b) are hysteretic and asymmetric. They also require a field of +0.15 T (−0.15 T) to reach magnetic saturation after biasing at positive (negative) field direction, implying more complicated switching behavior including a component of irreversible switching.

To fully resolve the magnetization process of the individual layers, XMCD hysteresis loops (Figs. 2(c) and 2(d)) were acquired by tuning the x-ray energy to the maximum XMCD signal at either the Mn or the Co L_3-edge and sweeping the field. The Mn XMCD minor loops were measured with the same biasing conditions as in the SQUID minor loops, while the Co XMCD loop was measured up to +/−1.4 T corresponding to the SQUID major loop. The coercivities from the Mn and Co XMCD loops match well with the two transition fields from the SQUID major loop. The Mn loops show biasing along the field axis with the same magnitude as the SQUID minor loops, which confirms the exchange coupling between the LSMO and LSCO layers. However, a much more pronounced hysteresis is observed in the Mn XMCD loops compared to the SQUID minor loops, indicating that irreversible switching of the soft LSMO layer is involved upon field reversal, unlike the case for exchange-spring system based on FM metals. In addition, the XMCD loops show smaller asymptotic behavior and reach magnetic saturation at a lower field (0.1 T) compared to the SQUID minor loops. We note that SQUID magnetometry measures the total magnetization of the sample, i.e., the contributions of both layers. The Co XMCD loop shows an initial sharp drop in XMCD magnitude at the transition field of the LSMO layer (∼0.002 T), it then reaches a plateau, and reverses completely at ∼1 T. The combination of SQUID minor and Mn XMCD loops suggests that the LSCO layer magnetization contributes to the minor loops to some extent. In other words, an interfacial portion of the LSCO layer rotates with the LSMO layer at small fields. The remainder of the LSCO layer requires a much larger field to switch directions.

The switching observed here deviates from the simple model that assumes a perfect rigid structure of the hard layer and reversible magnetization of the soft layer. It is generally believed that the soft layer moments rotate away from the hard layer with a reverse field and create a twisted structure along the thickness direction with an increasing rotation angle as the distance away from the interface increases. Fullerton *et al.* suggested that in the Sm-Co/Fe and Sm-Co/Co systems, a Bloch-like domain wall was formed in the plane parallel to the film surface and propagated from the soft layer into the hard as the reversal field increases.[6] In the case of the LSMO/LSCO bilayer, our results suggest that a Bloch-like domain wall propagates into an interfacial LSCO layer at a small field (∼0.002 T) separating it from the rigid part of the LSCO layer. Due to the finite probe depth of XMCD measurements (4 nm–10 nm),[26] the thickness of the interfacial LSCO layer can be estimated to be 1–2 unit cells based on the ratio (1/6th) of the initial magnetization drop of the Co XMCD loop to the total XMCD signal.

Previous reports have shown that interface roughness and electronic reconstruction via charge transfer both play significant roles in interfacial phenomena such as exchange coupling.[17,27] Interface roughness induced FM coupling, commonly known as "orange peel" coupling, is usually observed when the interface roughness exceeds 0.5 nm.[28,29] In this work, the bilayer sample shows an interface roughness value below 0.3 nm from XRR measurements so that "orange peel" coupling is believed to be negligible. Deviations from the bulk chemical structure were examined by XA spectroscopy at the Co and Mn $L_{2,3}$ edges (Figure 3). For comparison, XA spectra from single layer LSMO and LSCO films grown on LSAT substrates are also shown. Subtle differences in the XA spectra suggest changes in the Co and Mn valence states in the bilayer compared to the single layer films. The Mn L_3 peak for the bilayer (Fig. 3(a)) displays a shoulder feature 2.2 eV below the main peak, while the feature 1.6 eV below the main peak is less pronounced than in the single layer LSMO film. This feature is ascribed to an increase in Mn^{4+} concentration in the

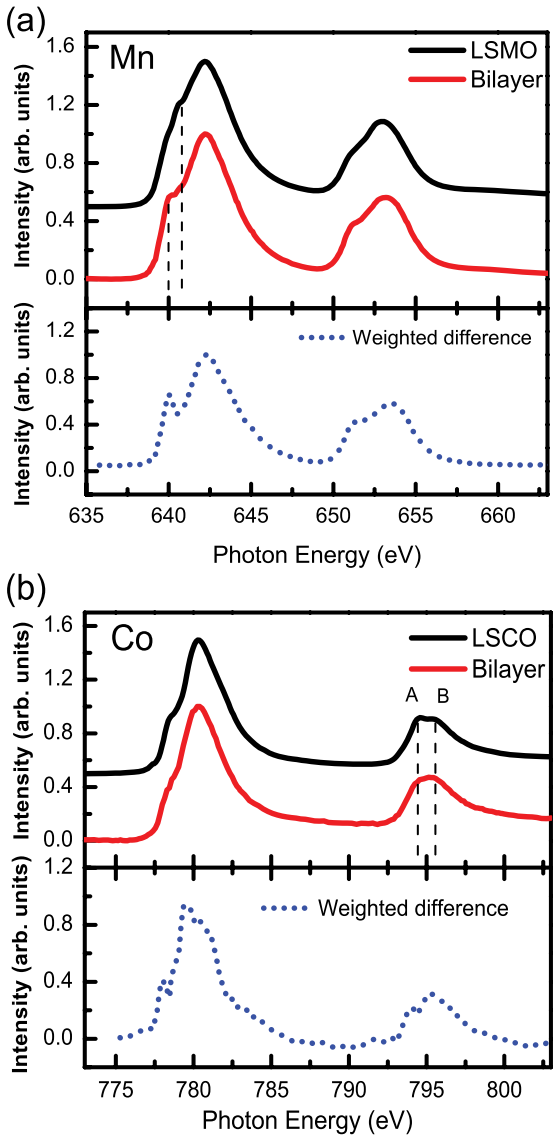

FIG. 3. XA spectra of the (a) Mn $L_{3,2}$ edges for the bilayer and single layer LSMO film (top panel), with the weighted difference curve (bottom panel). The dotted lines indicate shoulder features of Mn^{4+} and Mn^{3+} and (b) Co $L_{3,2}$ edges for the bilayer and single layer LSCO film (top panel), with the weighted difference curve (bottom panel). The dotted line indicates A/B sub-peaks on Co L_2 edge.

bilayer.[30] Subtle differences in the Co L_3 edge spectra can also be identified with a smaller A/B peak intensity ratio at the Co L_2 edge in the bilayer compared to the single layer LSCO film.

To provide a more quantitative analysis, the spectra from single layer films were rescaled and subtracted from the Mn and Co spectra of the bilayer. With scaling factors of 60% for Mn and 80% for Co, the calculated differences are shown in the bottom panels of Figure 3. The Mn difference curve strongly resembles the spectrum of octahedrally coordinated Mn^{4+} (e.g., Mn in $SrMnO_3$) with a prominent shoulder feature at ~1.7 eV below the main L_3 peak.[31] The Co difference curve shows more multiplet structures on the L_3 edge, and the overall line profile matches well with that of Co^{2+} in a similar octahedral bonding environment (e.g., as in $CoFe_2O_4$).[32] These results indicate an increase in Mn^{4+} concentration and the presence of Co^{2+} in the bilayer. We propose that the Co^{2+} and Mn^{4+} ions are mostly located at the interface. A charge redistribution process across the LSMO/LSCO interface is proposed here which involves an electron transfer from $Mn^{3+}$to Co^{3+} ($Mn^{3+} + Co^{3+} \rightarrow Mn^{4+} + Co^{2+}$). The FM coupling in each layer away from the interface is dominated by the double-exchange interaction between Mn^{4+} and Mn^{3+} or Co^{4+} and Co^{3+}, which contributes to the soft/hard behavior of LSMO/LSCO, respectively. Across the interface, the magnetic interactions are enriched due to the altered electronic structure with the coexistence of Co^{2+}, Co^{3+}, Co^{4+}, Mn^{3+}, and Mn^{4+} ions, where the Co ions are known to exist in multiple spin states[33] (i.e., low, intermediate, and high-spin configurations). The increase in Mn^{4+} concentration at the interface effectively pushes the LSMO system toward the case with higher Sr doping concentration, leading to FM properties with similar magnetic moment and slightly reduced Curie temperature.[13,34] In the interfacial LSCO layer, the large degree of freedom of the Co spin states induced by the charge transfer process results in magnetic properties that differ from single layer LSCO films. The presence of Co^{2+} could lead to interlayer coupling through a FM superexchange interaction along Mn^{4+}-O-Co^{2+} chains, as previously reported in the $La(Mn_xCo_{1-x})O_3$[31,35,36] and the double-perovskite La_2CoMnO_6.[37] Within the LSCO layer, additional indirect exchange interactions in the form of AFM superexchange through Co^{2+}-O-Co^{2+} and Co^{2+}-O-Co^{3+} chains[37] could exist as well. The wide spectrum of magnetic interactions at the interface favors a stronger exchange coupling of the interfacial LSCO layer to the LSMO layer than to the rigid part of LSCO layer. Therefore, the interfacial LSCO layer starts reversal with the LSMO layer at a much lower reversal field than the rigid part of the LSCO layer. The estimated thickness of this interface layer, i.e., 1–2 unit cells, matches reasonably well with the characteristic length scale of the charge transfer process, which is typically found to be a few unit cells in other perovskite systems such as $SrTiO_3$/$LaTiO_3$ and $LaMnO_3$/$SrMnO_3$.[38,39]

In conclusion, we report the observation of exchange-spring behavior in LSMO/LSCO bilayer thin films. The exchange coupling between LSCO and LSMO results in a biased minor hysteresis loop. The XMCD measurements show unexpected concurrent switching of the soft LSMO and an interface LSCO layer at fields that are well below the transition field of the hard LSCO layer. We propose a charge transfer scenario between Co and Mn ions at the interface that results in altered magnetic interactions. These results highlight the unique tunability of magnetic properties in complex oxide systems through indirect exchange interactions between transition metal ions that hold multiple valence/spin states, which are not commonly found in FM metal systems.

This work was supported by the Semiconductor Research Corporation under Task No. 2309.001. The ALS is supported by the Director, Office of Science, Office of Basic Energy Sciences, of the U.S. Department of Energy (DOE) under Contract No. DE-AC02-05CH11231. SSRL, a Directorate of SLAC National Accelerator Laboratory and an Office of Science User Facility, is operated for the U.S. DOE Office of Science by Stanford University. The authors thank Dr. Alpha T. N'Diaye for useful discussions on the XMCD data.

[1]J. Nogues and I. K. Schuller, J. Magn. Magn. Mater. **192**, 203 (1999).
[2]E. E. Fullerton, J. S. Jiang, and S. D. Bader, J. Magn. Magn. Mater. **200**, 392 (1999).
[3]M. Ghidini, G. Asti, R. Pellicelli, C. Pernechele, and M. Solzi, J. Magn. Magn. Mater. **316**, 159 (2007).
[4]R. Skomski and J. M. D. Coey, Phys. Rev. B **48**, 15812 (1993).
[5]E. F. Kneller and R. Hawig, IEEE Trans. Magn. **27**, 3588 (1991).
[6]E. E. Fullerton, J. S. Jiang, M. Grimsditch, C. H. Sowers, and S. D. Bader, Phys. Rev. B **58**, 12193 (1998).
[7]O. Hellwig, J. B. Kortright, K. Takano, and E. E. Fullerton, Phys. Rev. B **62**, 11694 (2000).
[8]D. Chumakov, R. Schäfer, D. Elefant, D. Eckert, L. Schultz, S. S. Yan, and J. A. Barnard, Phys. Rev. B **66**, 134409 (2002).
[9]J. U. Thiele, S. Maat, J. L. Robertson, and E. E. Fullerton, IEEE Trans. Magn. **40**, 2537 (2004).
[10]D. Suess, T. Schrefl, S. Fahler, M. Kirschner, G. Hrkac, F. Dorfbauer, and J. Fidler, Appl. Phys. Lett. **87**, 012504 (2005).
[11]E. Goto, N. Hayashi, T. Miyashit, and K. Nakagawa, J. Appl. Phys. **36**, 2951 (1965).
[12]J. E. Davies, O. Hellwig, E. E. Fullerton, J. S. Jiang, S. D. Bader, G. T. Zimanyi, and K. Liu, Appl. Phys. Lett. **86**, 262503 (2005).
[13]P. Zubko, S. Gariglio, M. Gabay, P. Ghosez, and J.-M. Triscone, Annu. Rev. Condens. Matter Phys. **2**, 141 (2011).
[14]E. Arenholz, G. van der Laan, F. Yang, N. Kemik, M. D. Biegalski, H. M. Christen, and Y. Takamura, Appl. Phys. Lett. **94**, 072503 (2009).
[15]E. Folven, A. Scholl, A. Young, S. T. Retterer, J. E. Boschker, T. Tybell, Y. Takamura, and J. K. Grepstad, Nano Lett. **12**, 2386 (2012).
[16]Y. Takamura, E. Folven, J. B. R. Shu, K. R. Lukes, B. Li, A. Scholl, A. T. Young, S. T. Retterer, T. Tybell, and J. K. Grepstad, Phys. Rev. Lett. **111**, 107201 (2013).
[17]X. Ke, M. S. Rzchowski, L. J. Belenky, and C. B. Eom, Appl. Phys. Lett. **84**, 5458 (2004).
[18]M. Ziese, I. Vrejoiu, E. Pippel, P. Esquinazi, D. Hesse, C. Etz, J. Henk, A. Ernst, I. V. Maznichenko, W. Hergert, and I. Mertig, Phys. Rev. Lett. **104**, 167203 (2010).
[19]V. K. Malik, C. Hieu Vo, E. Arenholz, A. Scholl, A. T. Young, and Y. Takamura, J. Appl. Phys. **113**, 153907 (2013).
[20]M. Sharma, J. Gazquez, M. Varela, J. Schmitt, and C. Leighton, Phys. Rev. B **84**, 024417 (2011).
[21]A. Bhattacharya and S. J. May, Annu. Rev. Mater. Res. **44**, 65 (2014).
[22]N. Kemik, M. Gu, F. Yang, C.-Y. Chang, Y. Song, M. Bibee, A. Mehta, M. D. Biegalski, H. M. Christen, N. D. Browning, and Y. Takamura, Appl. Phys. Lett. **99**, 201908 (2011).
[23]Leptos Manual (Bruker AXS, WI, 2005).
[24]M. Huijben, L. W. Martin, Y. H. Chu, M. B. Holcomb, P. Yu, G. Rijnders, D. H. A. Blank, and R. Ramesh, Phys. Rev. B **78**, 094413 (2008).
[25]M. A. Torija, M. Sharma, J. Gazquez, M. Varela, C. He, J. Schmitt, J. A. Borchers, M. Laver, S. El-Khatib, and C. Leighton, Adv. Mater. **23**, 2711 (2011).
[26]J. S. Lee, D. A. Arena, P. Yu, C. S. Nelson, R. Fan, C. J. Kinane, S. Langridge, M. D. Rossell, R. Ramesh, and C. C. Kao, Phys. Rev. Lett. **105**, 257204 (2010).
[27]M. Kiwi, J. Magn. Magn. Mater. **234**, 584 (2001).
[28]D. C. Parks, P. J. Chen, W. F. Egelhoff, and R. D. Gomez, J. Appl. Phys. **87**, 3023 (2000).
[29]D.-H. Han, J.-G. Zhu, and J. H. Judy, J. Appl. Phys. **81**, 4996 (1997).
[30]Y. Takamura, R. V. Chopdekar, E. Arenholz, and Y. Suzuki, Appl. Phys. Lett. **92**, 162504 (2008).
[31]T. Burnus, Z. Hu, H. H. Hsieh, V. L. J. Joly, P. A. Joy, M. W. Haverkort, H. Wu, A. Tanaka, H. J. Lin, C. T. Chen, and L. H. Tjeng, Phys. Rev. B **77**, 125124 (2008).
[32]R. V. Chopdekar, M. Liberati, Y. Takamura, L. F. Kourkoutis, J. S. Bettinger, B. B. Nelson-Cheeseman, E. Arenholz, A. Doran, A. Scholl, D. A. Muller, and Y. Suzuki, J. Magn. Magn. Mater. **322**, 2915 (2010).
[33]M. Merz, P. Nagel, C. Pinta, A. Samartsev, H. von Lohneysen, M. Wissinger, S. Uebe, A. Assmann, D. Fuchs, and S. Schuppler, Phys. Rev. B **82**, 174416 (2010).
[34]M. Izumi, Y. Konishi, T. Nishihara, S. Hayashi, M. Shinohara, M. Kawasaki, and Y. Tokura, Appl. Phys. Lett. **73**, 2497 (1998).
[35]P. A. Joy, Y. B. Khollam, and S. K. Date, Phys. Rev. B **62**, 8608 (2000).
[36]V. L. J. Joly, P. A. Joy, S. K. Date, and C. S. Gopinath, J. Phys.: Condens. Matter **13**, 649 (2001).
[37]R. I. Dass and J. B. Goodenough, Phys. Rev. B **67**, 014401 (2003).
[38]A. Ohtomo, D. A. Muller, J. L. Grazul, and H. Y. Hwang, Nature **419**, 378 (2002).
[39]S. Smadici, P. Abbamonte, A. Bhattacharya, X. Zhai, B. Jiang, A. Rusydi, J. N. Eckstein, S. D. Bader, and J. Zuo, Phys. Rev. Lett. **99**, 196404 (2007).